Cureus Journal of Engineering

Open Access Original Article

A Nonlocal Finite Element Approach for Nanobeams Based on Stress-Driven Model

Luciano Feo [1] , Gerarda Landi [1] , Giuseppe Lovisi [1] , Rosa Penna [1]

1. Civil Engineering, University of Salerno, Fisciano, ITA

Corresponding authors: Luciano Feo, lfeo@unisa.it, Gerarda Landi, gelandi@unisa.it, Giuseppe Lovisi, glovisi@unisa.it, Rosa Penna, rpenna@unisa.it

Received 04/22/2025
Review began 05/26/2025
Review ended 06/11/2025
Published 07/07/2025

DOI: https://doi.org/10.7759/s44388-025-05145-z

Abstract

The manuscript proposes a nonlocal finite element approach for the analysis of the bending behavior of Bernoulli-Euler nanobeams, based on well-posed Stress-Driven nonlocal continuum mechanics. The structural behavior of the nanobeams was investigated using COMSOL Multiphysics® 6.2. The approach is based on a 1D-finite element discrete model where the nonlocal constitutive law is introduced to capture the nonlocal effects characteristic of nanostructures, even though the software employs a classical local constitutive law by default. The proposed approach involves determining an elastic modulus multiplier function, ensuring equivalence between the bending curvature functions of the nonlocal and local models. The reliability and the potentialities of the proposed approach are assessed by comparing the numerical results with both experimental and analytical data available in the current literature. Additionally, the work performs a parametric investigation, presenting and examining the main results across different values of the nonlocal parameter, mesh type, and boundary conditions. This study offers a practical framework for the design of nanostructures using commercially available engineering software.

Categories: Structural Analysis and Finite Element Analysis, Nano Materials, Nanotechnology
Keywords: nonlocal finite element analysis, nanobeams, nonlocal effects, size effects, comsol multiphysics, boundary conditions.

Introduction

In recent decades, extraordinary advances in the fields of nanoscience and nanotechnology have driven the scientific community to concentrate its efforts on the analysis, modeling, and reliable design of nanostructures. These studies have fueled innovation, paving the way for sophisticated solutions and enhanced structural performance. Unlike macroscopic structures, understanding the size-dependent behavior of nanostructures is fundamental, considering their widespread application in emerging nanoengineering fields where nanosensors, nanoactuators, and nanomaterials are being increasingly used [1-7]. At the nanoscale, the mechanical response of nanostructures is governed by two primary size-dependent phenomena: small-scale effects, which account for long-range interactions within the nanostructure (bulk), and surface effects, resulting from the significant energy of surface atoms. Such phenomena, observable at the nanoscale, have been extensively validated through experimental studies and molecular dynamics simulations [8-13]. Nevertheless, conducting experimental tests at this scale is highly challenging and costly, while molecular dynamics simulations are computationally intensive and restricted to systems containing a limited number of atoms. Classical theories of elasticity fail to adequately describe these phenomena, posing significant challenges for accurate theoretical modeling. While experimental tests and molecular dynamics simulations provide valuable insights, predicting the behavior of nanostructures requires the development of advanced theoretical frameworks. For these reasons, it is necessary to resort to nonlocal elastic theories that can describe the structural behavior of nanostructures. In literature, the milestone of nonlocal elastic theories is represented by Eringen's integral model (i.e., strong form) and its equivalent differential formulation (i.e., weak form) [14,15]. Under this theory, the stress at each point in the solid is determined through a spatial convolution between local elastic strains with a bi-exponential kernel, which depends on the material's internal characteristic length. This model has been widely adopted in recent years to investigate the static and dynamic behavior of nanostructures [16-19]. Despite its extensive use, it has been shown that when applied to the analysis of nanostructures, the model leads to mathematical inconsistencies, often referred to as "nanomechanics paradoxes". These paradoxes arise from the incompatibility between the constitutive boundary conditions and the equilibrium equations [20-25]. To overcome this difficulty, Romano et al. [26] introduced the Stress-Driven nonlocal Model (SDM), mathematically well-posed and coherent for the study of nanostructures. This model is capable of capturing the consistent stiffening effect induced by the discrete nature of the material on small scales, influencing the static, instability, and dynamic responses of nanobeams [27-36]. Additionally, it represents a powerful tool for investigating nanobeams or nanofoundations [37], nanocomposite beams [38], and nanobeams made of functionally graded materials in hygrothermal environments [39]. It significantly contributes to the analysis of wave propagation in nanobeams [40,41]. Recently, Penna [42] integrated the SDM model with Gurtin and Murdoch's theory [43,44], originating the Surface Stress-Driven Model (SSDM) to examine how long-range interactions and surface energy influence the flexural behavior of functionally graded metal-ceramic nanobeams. The SSDM has been used to analyze the flexural response of Functionally Graded (FG) nanobeams in the presence of cracks [45], to analyze their free vibration response [46,47], and to explore the instability behavior [48] of FG nanobeams. Among the various methodologies employed to solve the governing differential equations in the structural analysis of nonlocal elastic nanostructures, the finite element method (FEM) has become increasingly prevalent. Renowned for its versatility, FEM excels in addressing challenges related to complex geometries, different material properties, boundary conditions, and applied loads, unlike other approaches or techniques. Significant emphasis has been placed in the literature on the advancement of nonlocal finite element formulations. Numerous nonlocal finite element analyses based on Eringen's theory have been proposed in recent years, like those that allow to study the free vibration [49] and buckling behavior of FG nanobeams [50] using first-order shear strain theory, as well as those that allow to study FG plates [51] using the third-order shear deformation theory of Reddy, to analyze composite laminated plates [52] and thin laminated nanoplates [53]. Recently, Pinnola et al. [54] introduced a nonlocal finite element formulation for nanobeams based on the Stress-Driven integral model, which leads to well-posed structural problems, unlike the Strain-Driven theory. It is important to note, as well known, that the finite element method is one of the most commonly implemented methods in commercial structural analysis software, as it allows for the analysis and resolution of complex engineering and physics problems. However, these computational tools implement the local theory, which means they cannot account for the small-scale effects characteristic of nanostructures. To overcome this limitation, the present work aims to develop an FEM approach that, once the finite element model is implemented using commercial software, is capable of capturing small-scale effects. The proposed approach yields results that align well with those of the closed-form SDM model across different boundary constraints and loading conditions. Therefore, the proposed FEM approach is able to capture the stiffening behavior of nanostructures dependent on size effects. The paper is structured as follows: the Stress-Driven Model for nanobeams is recalled first. Then, the type of finite element and mesh used, as well as the procedure for applying the proposed FEM approach, are described. To validate the proposed approach, the nonlocal parameter is calibrated using both the analytical solution of the SDM model and the proposed FEM approach, based on experimental data from the literature. The results of the parametric analysis are then examined, followed by some closing remarks (Table *1*).

Nomenclature	
L	Length of nanobeam
Σ	Generic cross-section
$\{O, x, y, z\}$	Cartesian coordinate system
O	Geometric center of Σ
x	Axis of nanobeam
y, z	Principal axes of geometric inertia of Σ
C	Elastic center of Σ
b, h	Width and thickness of rectangular cross-section
u_x	Component of the displacement field of the nanobeam along the x axis
u_y	Component of the displacement field of the nanobeam along the y axis
u_z	Component of the displacement field of the nanobeam along the z axis
w	Transverse displacement of the elastic center C
ε_{xx}	Axial strain of the nanobeam
$\delta \mathrm{U}$	Virtual strain energy
$\delta \mathrm{W}$	Virtual work of the external forces
σ_{xx}	Axial stress of the nanobeam
E	Young's modulus
ν	Poisson's ratio
ρ	Mass density
M	Bending moment
I_E	Bending stiffness

χ	Bending curvature
q_z	Transverse vertical distributed load
SDM	Stress-Driven Model
LBE	Local Bernoulli-Euler
L_c	Internal characteristic length
λ_c	Nonlocal parameter
Φ_{L_c}	Special kernel function
F	Concentrated vertical force
w_L	Local displacement
Ω	Domain of the nanobeam
Ω_e	e-th 1D-finite element
l_e	Length of the e-th finite element
u_e	Nodal displacement vector of the e-th finite element
v_i^e	Transverse displacement of the i-th node of Ω_e
φ_i^e	Rotation of the i-th node of Ω_e
χ_{SDM}	Nonlocal bending curvature function derived from the Stress-Driven Model
χ_L	Local bending curvature function
f_E	Elastic modulus multiplier function
$\widetilde{w}$	Dimensionless deflection
$\widetilde{w}_{SDM}$	Dimensionless deflection obtained using the SDM model
$\widetilde{w}_{FEM}$	Dimensionless deflection obtained using the FEM approach
$\Delta\%$	Percentage difference between the analytical solution and the FEM solution

TABLE 1: Nomenclature

Materials And Methods

Problem formulation

Governing Equations

Based on the Bernoulli-Euler theory, in the elastic coordinate reference system $\{C, x, y, z\}$, the Cartesian components of the displacement field of the nanobeam, along the x, y and z axes, respectively, can be written as follows:

$$u_x = -z\frac{\partial w(x)}{\partial x} \qquad (1a)$$

$$u_y = 0 \qquad (1b)$$

$$u_z = w(x) \qquad (1c)$$

where $w(x)$ is the transverse displacement of the elastic center C. In this case (homogenous nanobeam) the elastic center, C, coincides with the geometric center, O, of the nanobeam cross-section (Figure 1).

FIGURE 1: Coordinate system and configuration of a Bernoulli–Euler nanobeam

Consequently, the only nonzero kinematically compatible strain associated with the displacement field is the axial strain, defined as

$$\varepsilon_{xx} = -z\frac{\partial^2 w(x)}{\partial x^2} \tag{2}$$

By using the principle of virtual work, we can derive the governing equations, as follows:

$$\delta U + \delta W = 0 \tag{3}$$

being δU and δW are the virtual strain energy and virtual work done by external forces, respectively. The virtual strain energy is given by

$$\delta U = \int_0^L \int_\Sigma \sigma_{xx}\delta\varepsilon_{xx} d\Sigma dx = -\int_0^L M(x)\frac{\partial^2 \delta w}{\partial x^2}dx \tag{4}$$

where $\sigma_{xx} = \sigma_{xx}(z) = E\varepsilon_{xx}$, is the axial stress and $M = M(x)$ is the moment stress resultant, defined as follows:

$$M = \int_\Sigma z\sigma_{xx} d\Sigma = I_E \chi \tag{5}$$

where I_E denotes the bending stiffness and $\chi = \chi(x)$ is the elastic bending curvature.

The general expression of the bending stiffness, I_E , is given by the following equation

$$I_E = \int_\Sigma E z^2 d\Sigma \tag{6}$$

in which E denotes the elastic modulus of elasticity.

The expression of the virtual work of the external forces δW is

$$\delta W = -\int_0^L q_z \delta w dx \tag{7}$$

where $q_z = q_z(x) = q$ is the transverse vertical distributed load.

By substituting Equation (4) and Equation (7) into Equation (3) and applying the fundamental lemma of variational calculus, the equilibrium equation is derived as follows:

$$\frac{\partial^2 M}{\partial x^2} + q = 0 \tag{8}$$

The corresponding boundary conditions at the nanobeam's ends $x = 0, L$ can be determined by specifying one element from each of the two pairs of Standard (kinematic or static) Boundary Conditions, SBCs

$$w \quad or \quad \frac{\partial M}{\partial x} \tag{9a}$$

$$-\frac{\partial w}{\partial x} \quad or \quad M \tag{9b}$$

Stress-Driven Nonlocal Model

In this section, we provide a brief review of the SDM used to investigate the bending behavior of Bernoulli-Euler nanobeams as outlined in [27]. In accordance with the SDM, the constitutive relationship between the bending curvature, χ , and the bending moment, M , is defined by the following integral convolution

$$\chi(x) = \int_0^L \Phi_{L_c}(x-\overline{x}, L_c)(-\frac{M(\overline{x})}{I_E})d\overline{x} \tag{10}$$

where x and $\overline{x}$ are the position vectors of two points of the domain $[0, L]$, being L the nanobeam length; $L_c = \lambda_c L$ is the internal characteristic length that takes into account the nonlocal effects.

As is well-known, the expression of special kernel function, Φ_{L_c} , of Equation (10) which satisfy the properties of positivity, symmetry, limit impulsivity, and normalization on the real axis is given by

$$\Phi_{L_c}(x) = \frac{1}{2L_c}exp(-\frac{|x|}{L_c}) \tag{11}$$

Moreover, as argued in Ref. [26], the integral convolution in Equation (10) is equivalent to the following second-order differential equation

$$\left(1 - L_c^2\frac{\partial^2}{\partial x^2}\right)\chi = -\frac{M}{I_E} \tag{12}$$

if and only if the following two pairs of constitutive boundary conditions (CBCs) are satisfied at the nanobeam ends $(x = 0, L)$

$$\mp\frac{\partial\chi(0, L)}{\partial x}+\frac{1}{L_c}\chi(0, L) = 0 \tag{13}$$

The constitutive relations given in Equations (12) and (13) may be rewritten in terms of the nanobeam deflection, $w = w(x)$, by using the curvature-deflection relationship of the Bernoulli-Euler theory

$$\left(1 - L_c^2\frac{\partial^2}{\partial x^2}\right)\left(\frac{\partial^2 w}{\partial x^2}\right) = -\frac{M}{I_E} \tag{14}$$

$$\frac{\partial^3 w(0, L)}{\partial x^3}\mp\frac{1}{L_c}\frac{\partial^2 w(0, L)}{\partial x^2} = 0 \tag{15}$$

Bending Solution for Nanobeams with Different Boundary Conditions

In this subsection, we present the exact bending solutions for Bernoulli-Euler nanobeams with various boundary conditions, derived using the nonlocal SDM. Specifically, we consider five static configurations:

S1: Cantilever nanobeam subjected to concentrated force at the free end *(C-F,F)*;

S2: Cantilever nanobeam subjected to a transverse uniformly distributed load *(C-F,q)*;

S3: Simply-Supported nanobeam subjected to a transverse uniformly distributed load *(S-S,q)*;

S4: Clamped-Pinned nanobeam subjected to a transverse uniformly distributed load *(C-P,q)*;

S5: Clamped-Clamped nanobeam subjected to a transverse uniformly distributed load *(C-C,q)*.

The exact solutions of the nonlocal SDM are obtained from the differential problem (Equation 14) equipped with the constitutive boundary conditions (Equation 15). These solutions are consistent with those reported by Barretta et al. [27].

Cantilever nanobeam subjected to concentrated force at the free end: In this paragraph, the bending response of a cantilever nanobeam subjected to a concentrated force at the free end is derived using the Stress-Driven Model, employing Equations (14) and (15) and the boundary conditions shown in Figure 2.

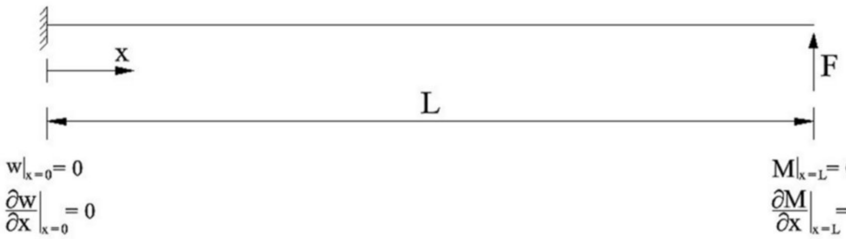

FIGURE 2: The static scheme of a Nanocantilever subject to a concentrated force F at the free end

The solution of the SDM differential problem provides the bending curvature for the nanocantilever

$$\chi(x) = \frac{F(L-x)}{I_E} - \frac{FL_c}{2I_E}e^{-x/L_c} + \frac{FL_c}{2I_E}e^{(x-L)/L_c} - \frac{FL}{2I_E}e^{-x/L_c} \tag{16}$$

which is the sum of the classical (local) curvature and a nonlocal curvature dependent on the internal characteristic length L_c .

The nonlocal deflection, w , is obtained by substituting the relationship between deflection and bending curvature into Equation (16) and is expressed in Equation (17).

$$w = w_L + \frac{FL_c\,e^{-(x+L)/L_c}}{2I_E}\begin{bmatrix} L_c^2(e^{x/L_c}-1)(e^{L/L_c + e^{x/L_c}}) - e^{(x+L)/L_c}Lx + \\ +L_c(-e^{L/L_c}L + e^{(x+L)/L_c}(L-x) - e^{x/L_c}x) \end{bmatrix} \tag{17}$$

where $w_L = w_L(x)$ is the classical (local) displacement of the nanocantilever

$$w_L = \frac{Fx^2}{6I_E}(3L - x) \tag{18}$$

Cantilever nanobeam subjected to a transverse uniformly distributed load: The bending response, obtained using the SDM, has also been calculated for the cantilever nanobeam subjected to a transverse uniformly distributed load, taking into account the boundary conditions presented in Figure 3.

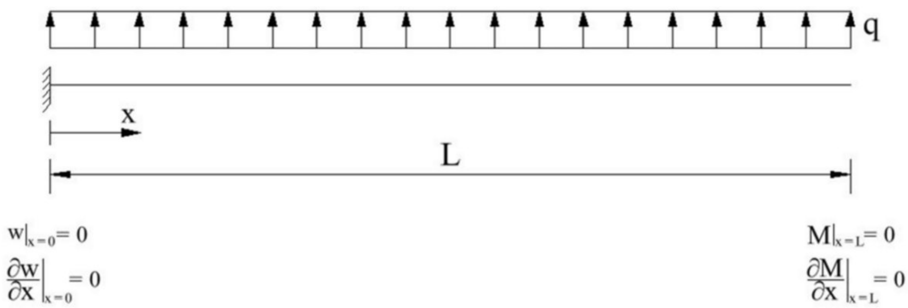

FIGURE 3: The static scheme of a Nanocantilever subject to a transverse uniformly distributed load q

The following equation expresses the bending curvature of the cantilever nanobeam

$$\chi(x) = -\frac{2qL_c^2\, e^{(x-L)/L_c} + q\, e^{-x/L_c}(2L_c^2 + 2L_cL + L^2) - 2q\left[2L_c^2 + (L-x)^2\right]}{4I_E} \quad (19)$$

which is the sum of the classical (local) curvature and the nonlocal curvature dependent on the internal characteristic length.

The nonlocal deflection, w, is expressed in the following equation

$$w = w_L + \frac{qL_c\, e^{-(x+L)/L_c}}{4I_E}\begin{bmatrix} 2L_c^3(e^{L/L_c} - e^{x/L_c})(e^{x/L_c} - 1) - e^{(x+L)/L_c}L^2x + \\ +2L_c^2(-e^{L/L_c}L + e^{(x+L)/L_c}(L-x) + e^{x/L_c}x) + \\ +L_ce^{L/L_c}((e^{x/L_c} - 1)L^2 - 2e^{x/L_c}Lx + 2e^{x/L_c}x^2) \end{bmatrix} \quad (20)$$

where $w_L = w_L(x)$ is the classical (local) displacement of the nanocantilever

$$w_L = \frac{qx^2(6L^2 - 4Lx + x^2)}{24I_E} \quad (21)$$

Simply-supported nanobeam subjected to a transverse uniformly distributed load: Through the application of the SDM, the bending response of the simply-supported nanobeam subjected to a transverse uniformly distributed load has also been determined, using the boundary conditions shown in Figure 4.

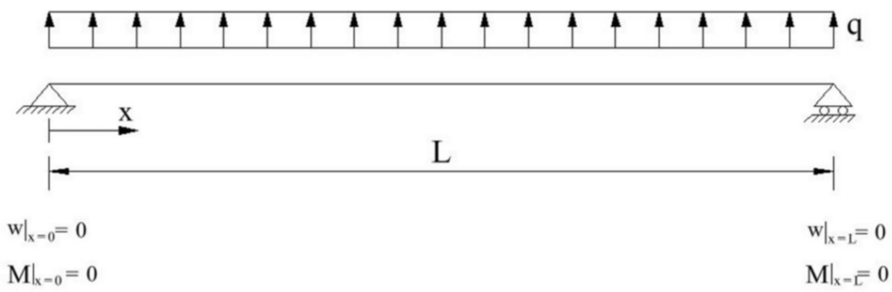

FIGURE 4: The static scheme of a simply-supported nanobeam subject to a transverse uniformly distributed load q

The bending curvature of the nanobeam is defined in the following equation

$$\chi(x) = -\frac{qL_c\, e^{-x/L_c}(2L_c + L) + qL_c\, e^{(x-L)/L_c}(2L_c + L) - 2q(2L_c^2 + x(L-x))}{4I_E} \quad (22)$$

which is the sum of the classical (local) curvature and a nonlocal curvature dependent on the internal characteristic length.

The nonlocal deflection, w , is given by Equation (23)

$$w = w_L + \frac{qL_c^2\, e^{-(x+L)/L_c}}{4I_E}\begin{bmatrix} 2L_c^2(e^{L/L_c} - e^{x/L_c})(e^{x/L_c} - 1) + \\ +L_cL(e^{L/L_c} - e^{x/L_c})(e^{x/L_c} - 1) + \\ -2e^{(x+L)/L_c}(L-x)x \end{bmatrix} \quad (23)$$

where $w_L = w_L(x)$ is the classical (local) displacement of the nanocantilever

$$w_L = \frac{qx(L^3 - 2Lx^2 + x^3)}{24I_E} \quad (24)$$

Clamped-pinned nanobeam subjected to a transverse uniformly distributed load: Using the SDM, the bending response of the clamped-pinned nanobeam subjected to a transverse uniformly distributed load has also been derived, employing the boundary conditions illustrated in Figure 5.

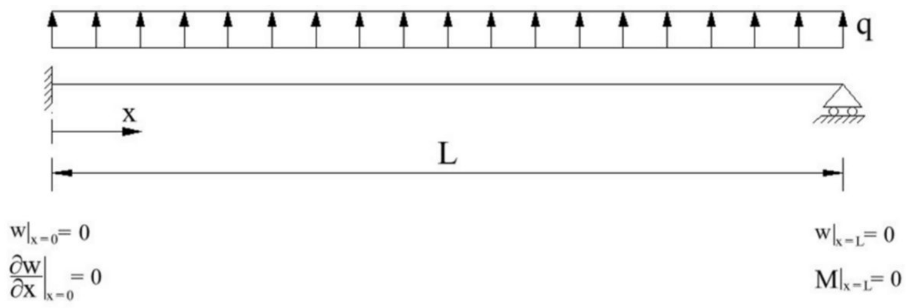

FIGURE 5: The static scheme of a clamped-pinned nanobeam subject to a transverse uniformly distributed load q

The lengthy expression for the transverse deflection is omitted in this case for brevity but for completeness we report the expression of the bending moment M

$$M = M_L + \frac{3qL_cL(L-x)}{8}\frac{6L_c^2(e^{L/L_c}-1)-2L_c(1+2e^{L/L_c}L)+e^{L/L_c}L^2}{6L_c^3(e^{L/L_c}-1)-6L_c^2L-3L_ce^{L/L_c}L^2+2e^{L/L_c}L^3} \quad (25)$$

where $M_L = M_L(x)$ is the classical (local) bending moment of the clamped-pinned nanobeam.

$$M_L = \frac{q(L^2-5Lx+4x^2)}{8} \quad (26)$$

Clamped-clamped nanobeam subjected to a transverse uniformly distributed load: The SDM application has also been used to determine the bending response of the clamped-clamped nanobeam subjected to a transverse uniformly distributed load, with the boundary conditions shown in Figure 6.

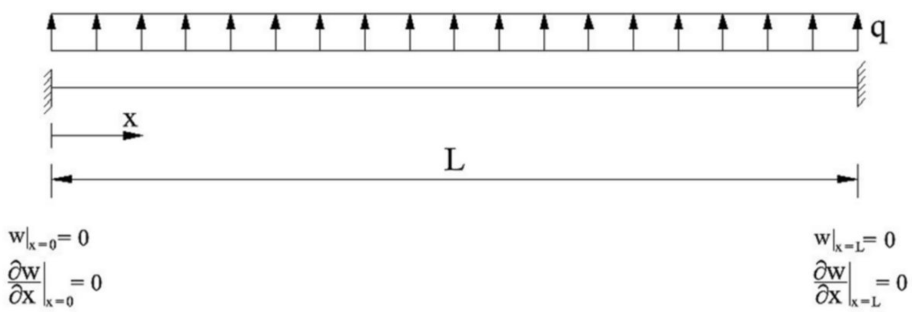

FIGURE 6: The static scheme of a clamped-clamped nanobeam subject to a transverse uniformly distributed load q

The expression of the nonlocal deflection, w , is represented in Equation (27)

$$w = w_L + \frac{1}{24I_E(L_c - L_c e^{L/L_c} + e^{L/L_c}L)}\left[\begin{array}{c} qL_ce^{-x/(L_cL)}(6L_c+L)(L_c(e^{L/L_c}-e^{x/L_c})(e^{x/L_c}-1)L+ \\ +e^{x/L_c}(e^{L/L_c}-1)x(x-L) \end{array}\right] \quad (27)$$

where $w_L = w_L(x)$ is the classical (local) displacement of the clamped-clamped nanobeam

$$w_L = \frac{qx^2(L-x)^2}{24I_E} \quad (28)$$

Finite element analysis

In this section, a 1D-finite element approach for the study of the size-dependent bending behavior of nanobeams is presented. The analysis has been developed by using the FEM COMSOL Multiphysics® 6.2 software.

Finite Element Approximation

The nanobeam domain, Ω , is discretized in *E* disjoint 1D-finite elements $\Omega_e =]x_e, x_{e+1}[$ $(e = \{1, 2\})$ with length l_e (Figure 7). The nodal displacement vector, $\mathbf{u}^e$, of the e-*th* finite element is defined as

$$\mathbf{u}^e = \begin{Bmatrix} v_1^e \\ \varphi_1^e \\ v_2^e \\ \varphi_2^e \end{Bmatrix} \tag{29}$$

being v_i^e and φ_i^e the transverse displacement and rotation of the *i-th* node $(i = 1, 2)$ of Ω_e . Note that the displacement field across the region is interpolated using cubic Lagrange shape functions, ensuring a smooth approximation of the nanobeam's deformation.

Two different finite element meshes have been considered for the analysis in order to investigate the influence of the mesh density on the accuracy of the FEM approach: Mesh 1, with $E = 2$, and Mesh 2, with $E = 10$.

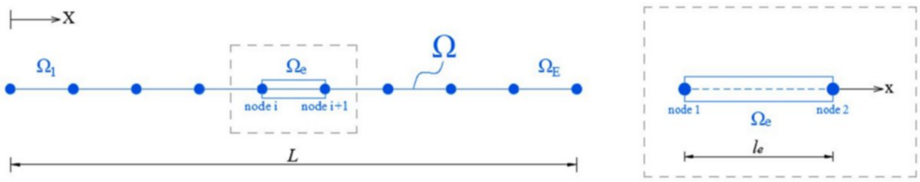

FIGURE 7: Finite element discretization of nanobeam and e-th finite element with corresponding degrees of freedom

Material Constitutive Modeling

By default, the material library in COMSOL Multiphysics® 6.2 applies a local constitutive law, which is insufficient for capturing small-scale effects. To overcome this limitation, this study introduces a FEM approach designed to incorporate the characteristic nonlocal effects of nanostructures, even though the model's software inherently uses a local constitutive law. The proposed approach involves determining an elastic modulus multiplier function, f_E , which ensures the equality between the expressions of the bending curvature functions of the local (LBE) and nonlocal models (SDM). The procedure for identifying this multiplier function is outlined in the flow chart presented in Table 2.

Flow chart of the solution procedure of the proposed FEM approach
STEP 1. Calculation of the nonlocal analytical solution. The nonlocal analytical solution is derived from the Stress-Driven Model (SDM) using the differential formulation, as expressed in Equations (14, 15).
STEP 2. Calculation of the local analytical solution. The local analytical solution is obtained using the classical Euler-Bernoulli elasticity theory.
STEP 3. Identification of the elastic modulus multiplier function (f_E). The elastic modulus multiplier function, f_E, is obtained imposing the equivalence between the nonlocal and local bending curvature functions: $\chi_{SDM}(x) - \chi_L(x) = 0$ where $\chi_{SDM}(x) = \chi(x)$ represents the nonlocal bending curvature function derived from the Stress-Driven Model, and $\chi_L = \chi_L(x)$ is the local bending curvature function.
STEP 4. Modeling the nanobeam in COMSOL Multiphysics®. Definition of the geometrical characteristics and mechanical properties of the nanobeam mesh elements in COMSOL Multiphysics® and imposition of the boundary conditions at the nanobeam's ends. Ensure that the elastic modulus in the finite element model is equal to the product of the material's intrinsic elastic modulus and the multiplier function f_E.
STEP 5. Analysis. Finite element simulation and validation of the proposed approach through comparison with analytical and experimental results in the literature.

TABLE 2: Flow chart of the solution procedure of the proposed FEM approach

FEM, finite element method

The analytical expressions of the elastic modulus multiplier functions, f_E, for the five static configurations are given in Appendix A.

In the following figures (Figures 8-12), the graph of the elastic modulus multiplier function, f_E, across the nanobeam axis of the five static configurations of the current study are plotted.

In each case, the nonlocal parameter λ_c varies within the set $0.01, 0.03, 0.05, 0.07, 0.10$.

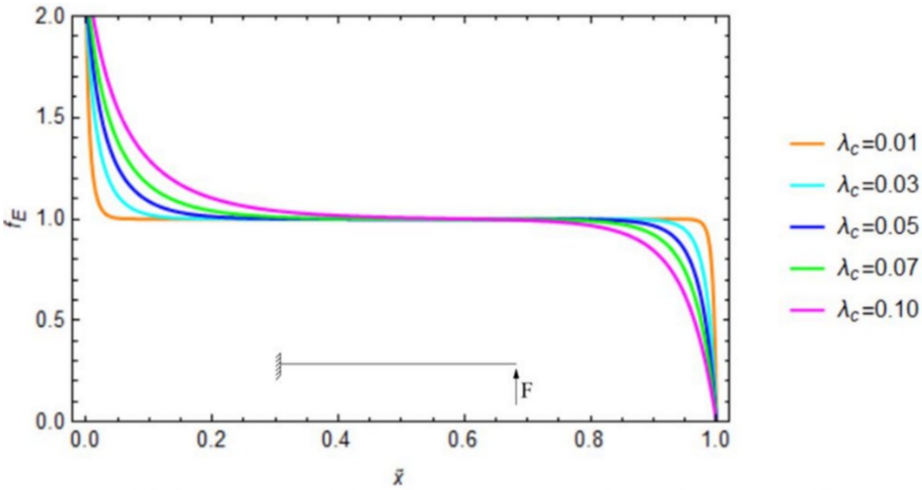

(a) S1: Cantilever nanobeam subjected to concentrated force at the free end ($C-F, F$).

FIGURE 8: Plots of elastic modulus multiplier function, varying the nonlocal parameter λc in the set λc = {0.01,0.03,0.05,0.07,0.10} for Cantilever nanobeam subjected to concentrated force at the free end (C-F,F)

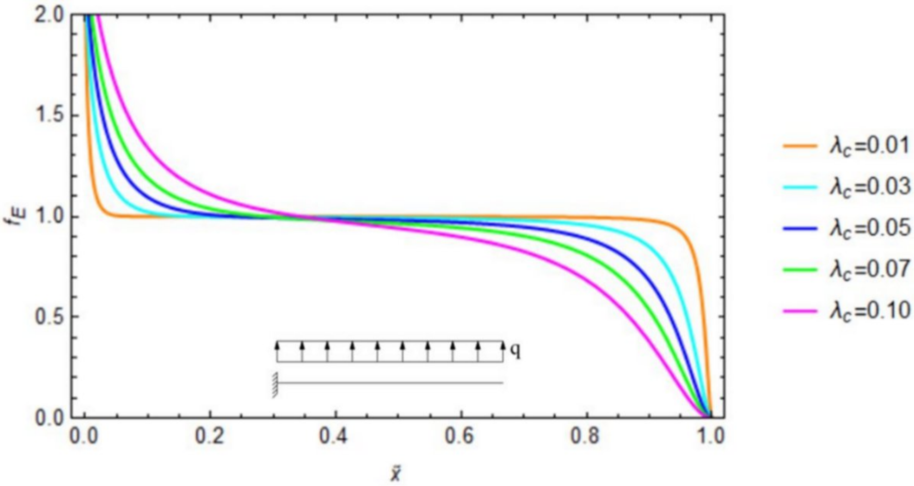

(b) S2: Cantilever nanobeam subjected to a transverse uniformly distributed load $(C - F, q)$.

FIGURE 9: Plots of elastic modulus multiplier function, varying the nonlocal parameter λc in the set λc = {0.01,0.03,0.05,0.07,0.10} for Cantilever nanobeam subjected to a transverse uniformly distributed load (C-F,q)

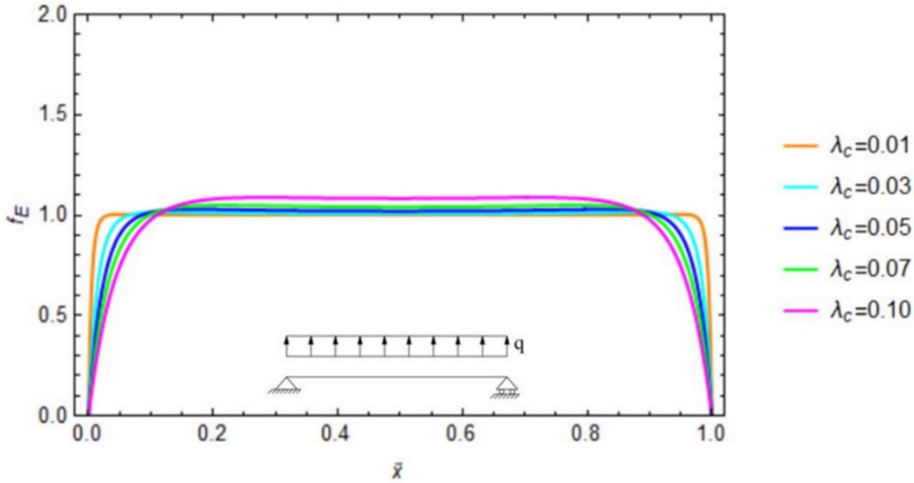

(c) S3: Simply-Supported nanobeam subjected to a transverse uniformly distributed load $(S - S, q)$.

FIGURE 10: Plots of elastic modulus multiplier function, varying the nonlocal parameter λc in the set λc = {0.01,0.03,0.05,0.07,0.10} for simply-supported nanobeam subjected to a transverse uniformly distributed load (S-S,q)

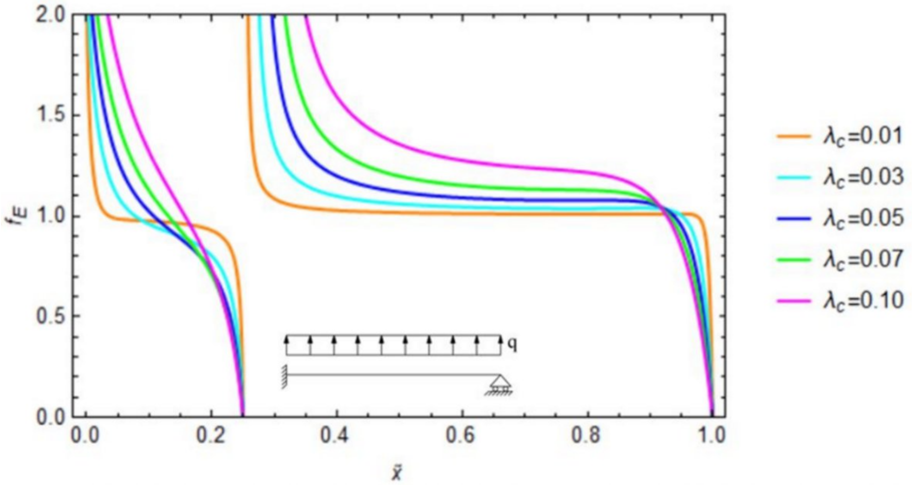

(d) S4: Clamped-Pinned nanobeam subjected to a transverse uniformly distributed load $(C-P,q)$.

FIGURE 11: Plots of elastic modulus multiplier function, varying the nonlocal parameter λc in the set λc = {0.01,0.03,0.05,0.07,0.10} for clamped-pinned nanobeam subjected to a transverse uniformly distributed load (C-P,q)

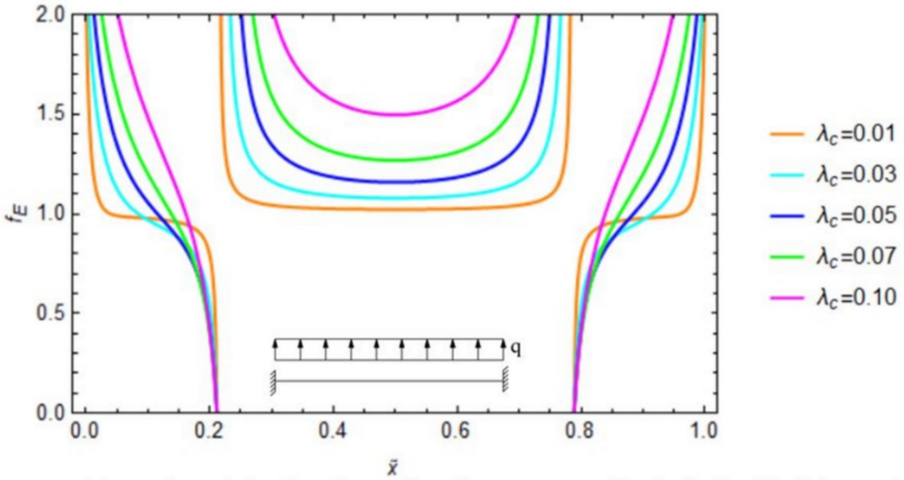

(e) S4: Clamped-Pinned nanobeam subjected to a transverse uniformly distributed load $(C-P,q)$.

FIGURE 12: Plots of elastic modulus multiplier function, varying the nonlocal parameter λc in the set λc = {0.01,0.03,0.05,0.07,0.10} for clamped-clamped nanobeam subjected to a transverse uniformly distributed load (C-C,q)

Results

Validation of the proposed FEM approach

In order to validate the numerical results, the nonlocal parameter was calibrated by both the analytical solution of the SDM model (Equations 14 and 15) and the proposed FEM approach, using the experimental data provided by Darban et al. [32].

According to Darban et al. [32], quasi-static bending tests were performed on microcantilevers subjected to a transverse point load applied at the free end (see Figure *13*). The microbeams varied in length, had a constant thickness-to-length ratio of h/L = 10, and a width of b = 235 mm. They were composed of epoxy resin, with a Young's modulus and Poisson's ratio υ = 0.38. These experiments were simulated in both the analytical (SDM) and the FEM approaches as microcantilevers under plane stress conditions, where the bending stiffness is given by $I_E = \frac{Ebh^3}{12}$. The experimental results were specifically obtained for microcantilevers of three different lengths: L = 1150, 380, and 200 mm, and are shown in Figures *14*-*16* with red circular markers.

Using the FEM approach with Mesh 1, it was found that a finite element solution aligning with the experimental results is achieved with a value set to 135 mm.

The load-displacement curves derived from the FEM approach are presented in Figures *14*-*16* for cases of L_c = 0 (magenta circular markers) and L_c = 135 mm (blue circular markers). Additionally, the figures include load-displacement curves calculated using SDM theory for L_c = 0 mm (local solution) and L_c = 135 mm, represented by black and green lines, respectively.

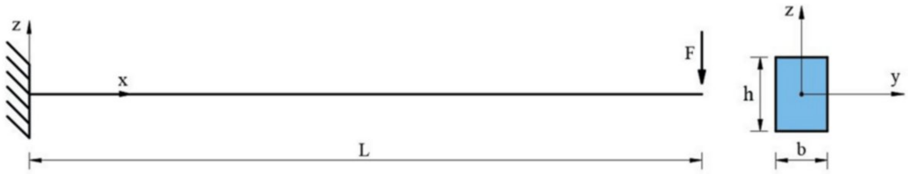

FIGURE 13: Coordinate system and configuration of the microcantilever

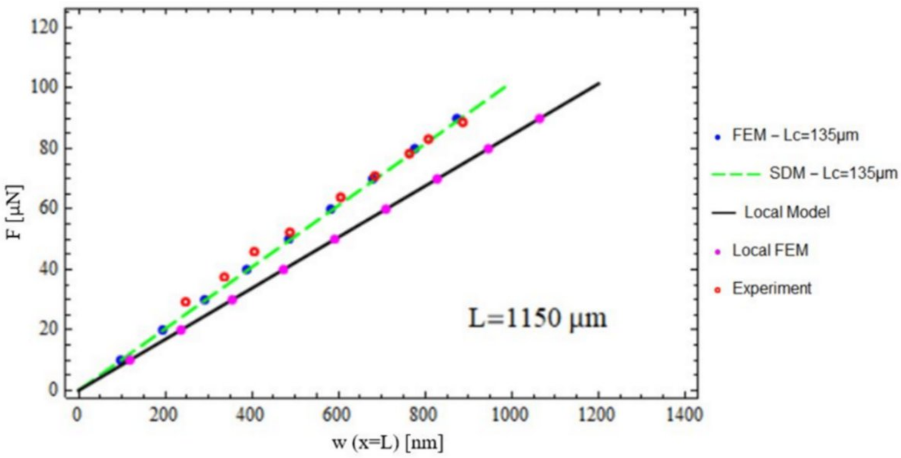

FIGURE 14: Comparison of experimental, analytical and FEM results in the form of load-displacement curves for epoxy microcantilevers of length 1150 microns

FEM, finite element method; SDM, Stress-Driven nonlocal Model

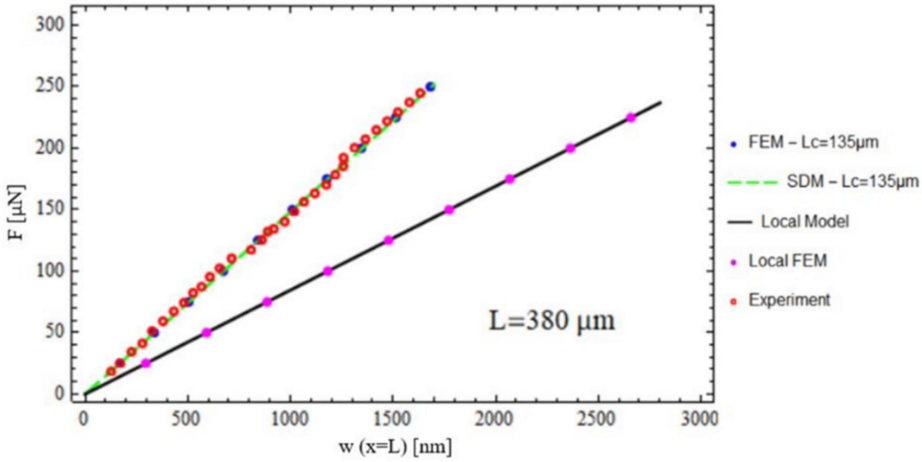

FIGURE 15: Comparison of experimental, analytical, and FEM results in the form of load-displacement curves for epoxy microcantilevers of length 380 microns

FEM, finite element method; SDM, Stress-Driven nonlocal Model

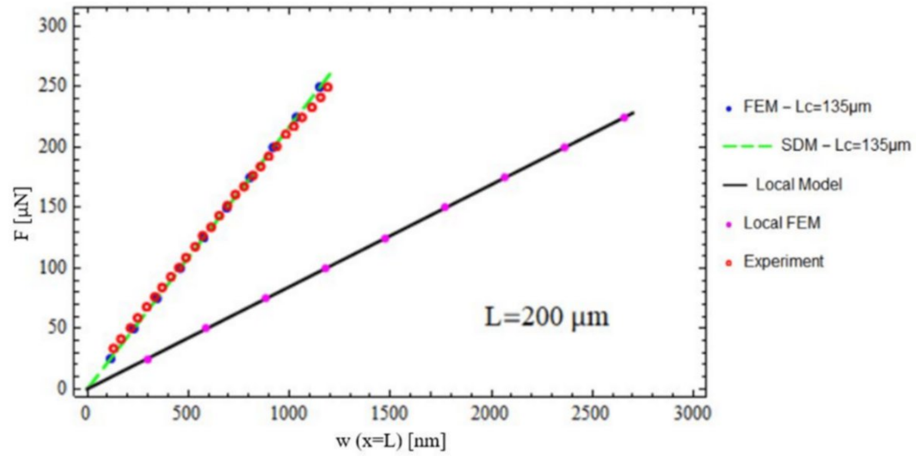

FIGURE 16: Comparison of experimental, analytical and FEM results in the form of load-displacement curves for epoxy microcantilevers of length 200 microns.

FEM, finite element method; SDM, Stress-Driven nonlocal Model

It was shown that the value of the nonlocal parameter value required to calibrate the FEM approach to the experimental data is consistent with the nonlocal parameter obtained in Ref. [32] for calibrating the analytical solution against experimental results. In conclusion, the current approach was validated by comparing the load-displacement curves obtained with the FEM approach with those derived by Darban et al. [32].

Discussion

In this section, a FEM analysis of the bending response of Bernoulli-Euler nanobeams with L = 10 nm and with square cross-section (thickness h = 0.1 L and width $h = b$) was conducted, taking into account five static configurations described in the previous section.

The characteristic values of the material's physical and elastic properties, specifically Young's modulus, E, mass density, ρ, and Poisson's ratio, ν, are summarized in Table 3.

Material	Parameters	Values	Unit
Metal (Al)	E	70	(GPa)
	ρ	2700	(kg/m^3)
	v	0.30	(-)

TABLE 3: Physical and elastic properties of the material of nanobeams

Moreover, the results obtained using the approach FEM proposed in "Finite element analysis" section are analyzed and compared with the analytical solutions given by Stress-Driven Model ("Problem formulation" section). The results obtained using the SDM model are the same of those presented in [27].

For each static scheme, the results are presented in terms of dimensionless deflection, defined as $\tilde{w} = \frac{w\, I_E}{F L^3}\; or\; \tilde{w} = \frac{w\, I_E}{q L^4}$, depending on the applied load type.

Tables 4-7 summarize the results of the numerical analysis in terms of the dimensionless deflection, corresponding to $\lambda_c = \{0.00, 0.01, 0.02, 0.03, 0.04, 0.05, 0.06, 0.07, 0.08, 0.09, 0.10\}$. In particular, the results obtained using Mesh 1 are presented in Tables 4 and 5, while those obtained with Mesh 2 are shown in Tables 6 and 7. In these tables, the percentage difference between the analytical solution and the FEM solution is represented by the symbol Δ (%) and is calculated using Equation (30).

$$\Delta(\%) = \frac{\widetilde{w}_{SDM} - \widetilde{w}_{FEM}}{\widetilde{w}_{SDM}} \cdot 100 \qquad (30)$$

where $\tilde{w}_{\mathrm{SDM}}$ and $\tilde{w}_{\mathrm{FEM}}$ represent the dimensionless deflection obtained using the SDM model and FEM approach, respectively.

λ_c		$\widetilde{w}$						
		C-F, F				C-F, q		
		ξ = 1				ξ = 1		
		SDM	FEM-q	Δ (%)		SDM	FEM-q	Δ (%)
0.00^+		0.33333	0.33333	0.00000		0.12500	0.12500	0.00000
0.01		0.32833	0.33201	1.11867		0.12253	0.12439	1.52481
0.02		0.32334	0.32545	0.65340		0.12010	0.12126	0.96909
0.03		0.31836	0.31843	0.02111		0.11773	0.11790	0.15242
0.04		0.31340	0.31206	0.42603		0.11540	0.11488	0.44731
0.05		0.30846	0.30624	0.71790		0.11313	0.11216	0.85402
0.06		0.30355	0.30082	0.89886		0.11090	0.10966	1.11590
0.07		0.29868	0.29568	1.00176		0.10873	0.10734	1.27127
0.08		0.29385	0.29076	1.05044		0.10660	0.10516	1.34976
0.09		0.28906	0.28599	1.06234		0.10453	0.10309	1.37441
0.10		0.28433	0.28135	1.04986		0.10250	0.10110	1.36238

TABLE 4: Dimensionless deflection for the following nanobeam configurations: C-F,F and C-F,q, varying the nonlocal parameter in the set λc = {0.00, 0.01, 0.02, 0.03, 0.04, 0.05, 0.06, 0.07, 0.08, 0.09, 0.10} for both SDM and FEM solutions (Mesh 1)

SDM, Stress-Driven Nonlocal Model; FEM, finite element method

λ_c	$\widetilde{w}$								
	S-S, q			C-P, q			C-C, q		
	ξ = 1/2			ξ = 1/2			ξ = 1/2		
	SDM	FEM-q	Δ (%)	SDM	FEM-q	Δ (%)	SDM	FEM-q	Δ (%)
0.00^+	0.01302	0.01301	0.09312	0.00521	0.00521	0.00000	0.00260	0.00260	0.00000
0.01	0.01301	0.01301	0.00093	0.00508	0.00518	1.80849	0.00250	0.00258	3.39641
0.02	0.01297	0.01298	0.01975	0.00495	0.00503	1.58349	0.00239	0.00247	3.41922
0.03	0.01292	0.01292	0.04565	0.00481	0.00485	0.89120	0.00227	0.00233	2.53054
0.04	0.01284	0.01285	0.06696	0.00465	0.00467	0.25464	0.00215	0.00219	1.63761
0.05	0.01274	0.01275	0.08246	0.00450	0.00449	0.27106	0.00203	0.00205	0.86800
0.06	0.01263	0.01264	0.09312	0.00434	0.00431	0.69699	0.00192	0.00192	0.23847
0.07	0.01251	0.01252	0.10009	0.00417	0.00413	1.03698	0.00180	0.00180	0.26512
0.08	0.01237	0.01238	0.10429	0.00401	0.00396	1.30468	0.00169	0.00168	0.65698
0.09	0.01222	0.01223	0.10647	0.00385	0.00379	1.51428	0.00158	0.00157	0.95552
0.10	0.01207	0.01208	0.10726	0.00369	0.00363	1.68049	0.00148	0.00147	1.17997

TABLE 5: Dimensionless deflection for the following nanobeam configurations: S-S,q; C-P,q; C-C,q, varying the nonlocal parameter in the set λc = {0.00, 0.01, 0.02, 0.03, 0.04, 0.05, 0.06, 0.07, 0.08, 0.09, 0.10} for both SDM and FEM solutions (Mesh 1)

SDM, Stress-Driven Nonlocal Model; FEM, finite element method

λ_c	$\widetilde{w}$					
	C-F, F			C-F, q		
	ξ = 1			ξ = 1		
	SDM	FEM-q	Δ (%)	SDM	FEM-q	Δ (%)
0.00^+	0.33333	0.33333	0.00000	0.12500	0.12500	0.00000
0.01	0.32833	0.33279	0.12449	0.12253	0.12232	0.16993
0.02	0.32334	0.32285	0.15292	0.12010	0.11985	0.21186
0.03	0.31836	0.31803	0.10540	0.11773	0.11755	0.14780
0.04	0.31340	0.31318	0.06879	0.11540	0.11529	0.09724
0.05	0.30846	0.30383	0.04596	0.11313	0.11305	0.06550
0.06	0.30355	0.30345	0.03190	0.11090	0.11085	0.04577
0.07	0.29868	0.29861	0.02303	0.10873	0.10869	0.03325
0.08	0.29385	0.29380	0.01717	0.10660	0.10657	0.02494
0.09	0.28906	0.28902	0.01322	0.10453	0.10451	0.01928
0.10	0.28433	0.28430	0.01041	0.10250	0.10248	0.01525

TABLE 6: Dimensionless deflection for the following nanobeam configurations: C-F,F and C-F,q, varying the nonlocal parameter in the set λc = {0.00, 0.01, 0.02, 0.03, 0.04, 0.05, 0.06, 0.07, 0.08, 0.09, 0.10} for both SDM and FEM solutions (Mesh 2)

SDM, Stress-Driven Nonlocal Model; FEM, finite element method

λ_c	$\widetilde{w}$								
	S-S, q			C-P, q			C-C, q		
	ξ = 1/2			ξ = 1/2			ξ = 1/2		
	SDM	FEM-q	Δ (%)	SDM	FEM-q	Δ (%)	SDM	FEM-q	Δ (%)
0.00^+	0.01302	0.01302	0.00000	0.00521	0.00521	0.00000	0.00260	0.00260	0.00000
0.01	0.01301	0.01301	0.00006	0.00508	0.00507	0.19803	0.00250	0.00249	0.36804
0.02	0.01297	0.01297	0.00019	0.00495	0.00494	0.27278	0.00239	0.00237	0.52169
0.03	0.01292	0.01292	0.00028	0.00481	0.00480	0.20800	0.00227	0.00226	0.41066
0.04	0.01284	0.01284	0.00026	0.00465	0.00465	0.15677	0.00215	0.00216	0.30501
0.05	0.01274	0.01274	0.00022	0.00450	0.00449	0.17018	0.00203	0.00203	0.23039
0.06	0.01263	0.01263	0.00019	0.00434	0.00433	0.04803	0.00192	0.00191	0.17693
0.07	0.01251	0.01251	0.00014	0.00417	0.00417	0.04842	0.00180	0.00180	0.14039
0.08	0.01237	0.01237	0.00009	0.00401	0.00401	0.04110	0.00169	0.00169	0.11288
0.09	0.01222	0.01222	0.00007	0.00385	0.00385	0.03439	0.00158	0.00158	0.09129
0.10	0.01207	0.01207	0.00004	0.00369	0.00369	0.03201	0.00148	0.00148	0.07531

TABLE 7: Dimensionless deflection for the following nanobeam configurations: S-S,q; C-P,q; C-C,q, varying the nonlocal parameter in the set λc = {0.00, 0.01, 0.02, 0.03, 0.04, 0.05, 0.06, 0.07, 0.08, 0.09, 0.10} for both SDM and FEM solutions (Mesh 2)

SDM, Stress-Driven Nonlocal Model; FEM, finite element method

Figures *17*-*21* and Figures *22*-*26* present a comparison of the dimensionless deflection, $\widetilde{w}$, obtained using the FEM approach and SDM model for various loading conditions and boundary conditions. Specifically, Figures *17*-*21* show the results for the case of Mesh 1, while Figures *22*-*26* present the results for the case of Mesh 2. This comparison allows an evaluation of the effectiveness and consistency of the proposed approach across different mesh configurations in identical operating conditions. In these illustrations, the nonlocal parameter varies within the set {0.01, 0.03, 0.05, 0.10}. The Classical Local Model, represented by the black line, is recovered as λ_c tends to 0.00^+.

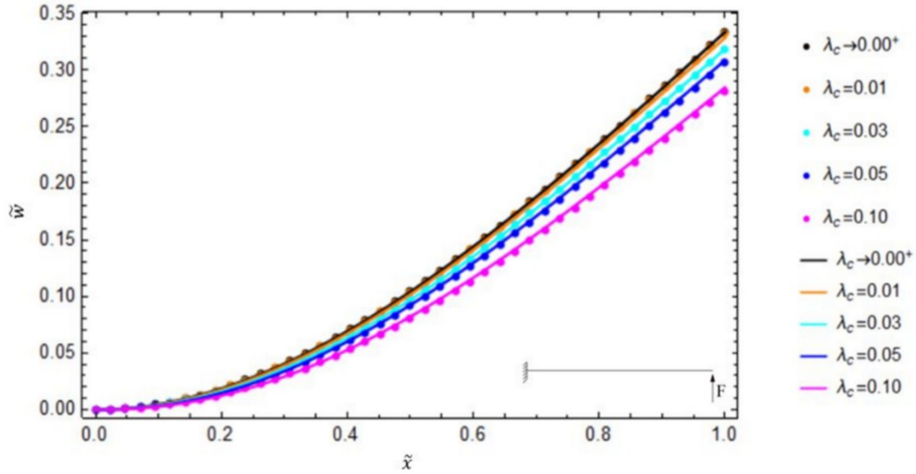

FIGURE 17: Comparison of analytical and the FEM results (Mesh 1) in terms of the dimensionless nonlocal deflection for different values of the nonlocal parameter and for the case of C-F,F

FEM, finite element method

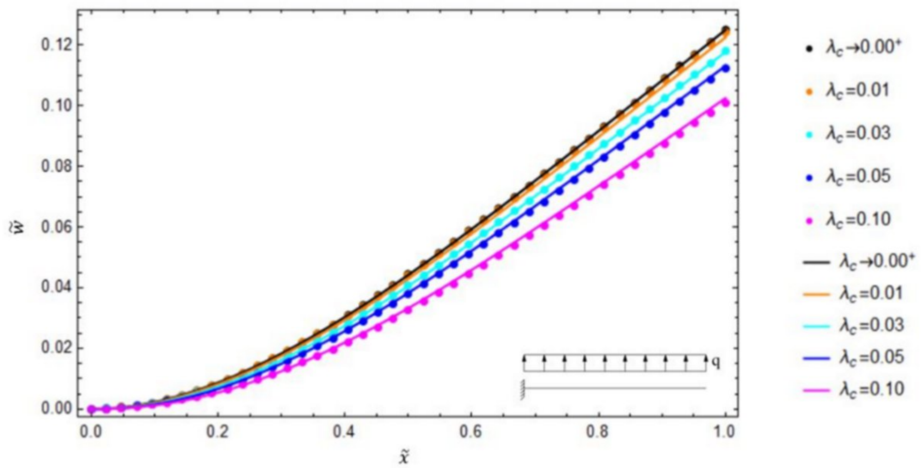

FIGURE 18: Comparison of analytical and the FEM results (Mesh 1) in terms of the dimensionless nonlocal deflection for different values of the nonlocal parameter and for the case of C-F,q

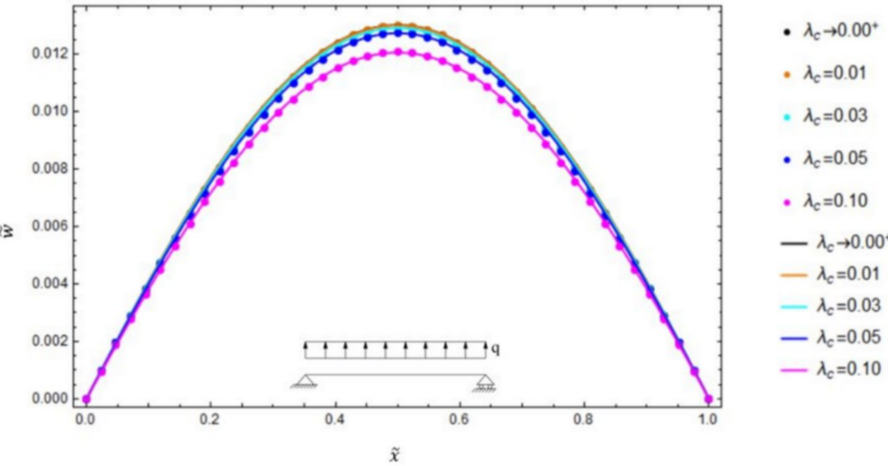

FIGURE 19: Comparison of analytical and the FEM results (Mesh 1) in terms of the dimensionless nonlocal deflection for different values of the nonlocal parameter and for the case of S-S,q

FEM, finite element method

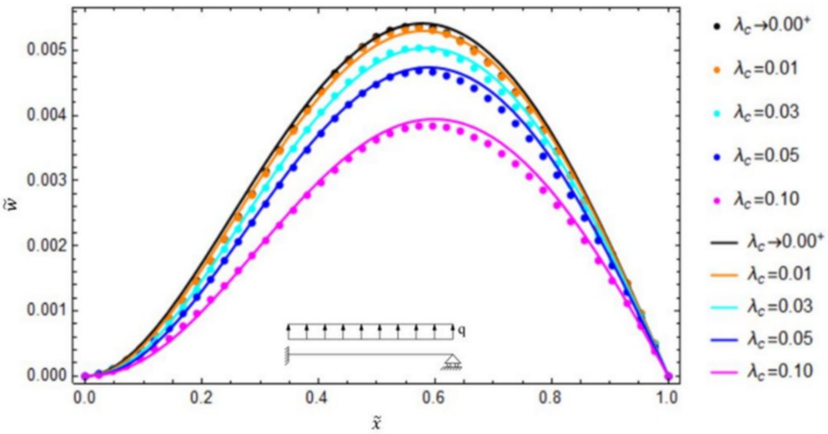

FIGURE 20: Comparison of analytical and the FEM results (Mesh 1) in terms of the dimensionless nonlocal deflection for different values of the nonlocal parameter and for the case of C-P,q

FEM, finite element method

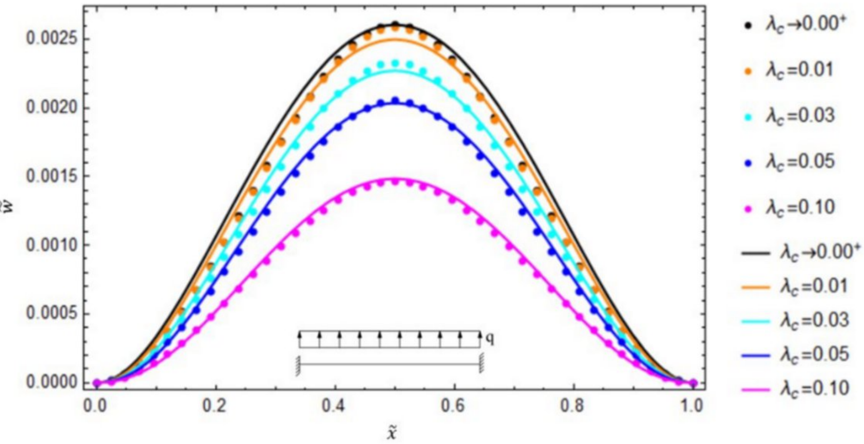

FIGURE 21: Comparison of analytical and the FEM results (Mesh 1) in terms of the dimensionless nonlocal deflection for different values of the nonlocal parameter and for the case of C-C,q

FEM, finite element method

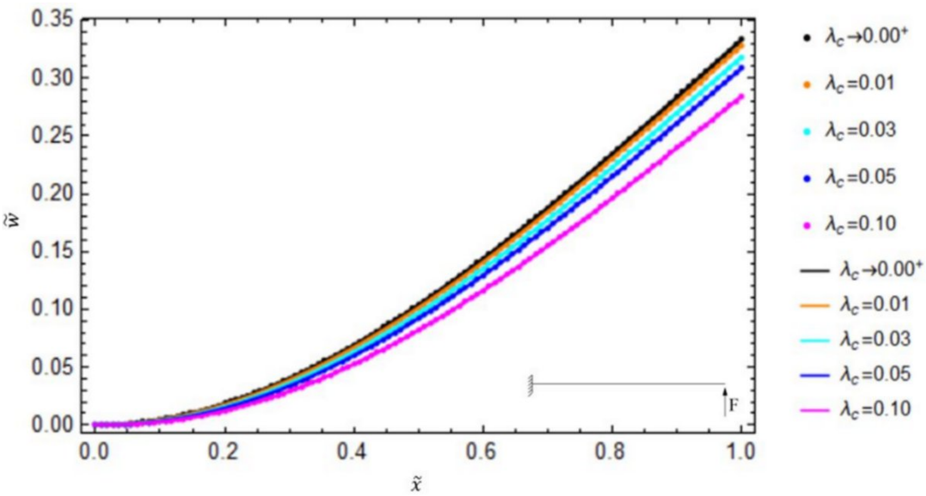

FIGURE 22: Comparison of analytical and the FEM results (Mesh 2) in terms of the dimensionless nonlocal deflection for different values of the nonlocal parameter and for the case of C-F,F

FEM, finite element method

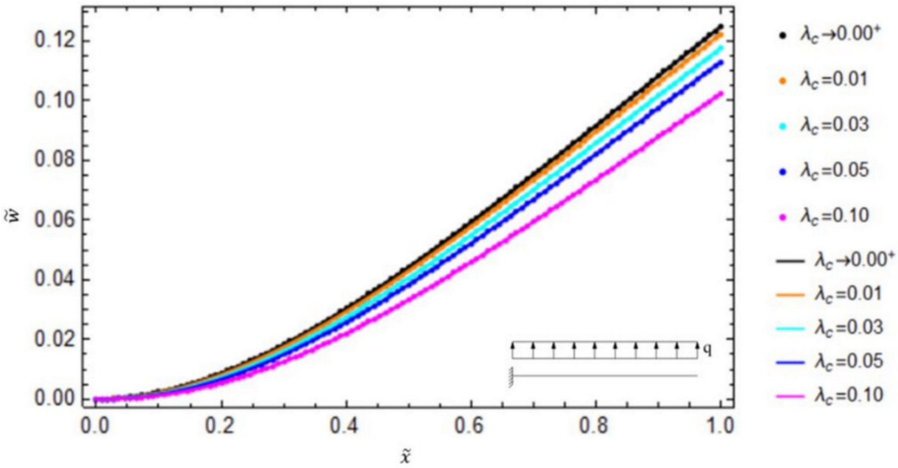

FIGURE 23: Comparison of analytical and the FEM results (Mesh 2) in terms of the dimensionless nonlocal deflection for different values of the nonlocal parameter and for the case of C-F,q

FEM, finite element method

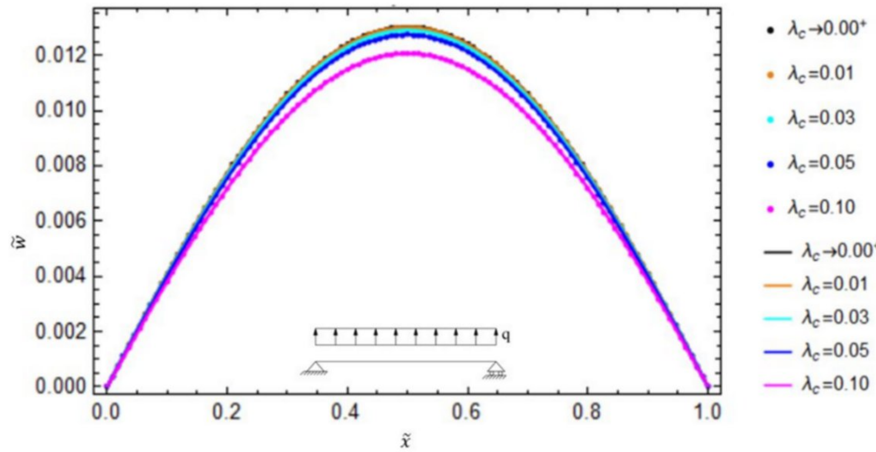

FIGURE 24: Comparison of analytical and the FEM results (Mesh 2) in terms of the dimensionless nonlocal deflection for different values of the nonlocal parameter and for the case of S-S,q

FEM, finite element method

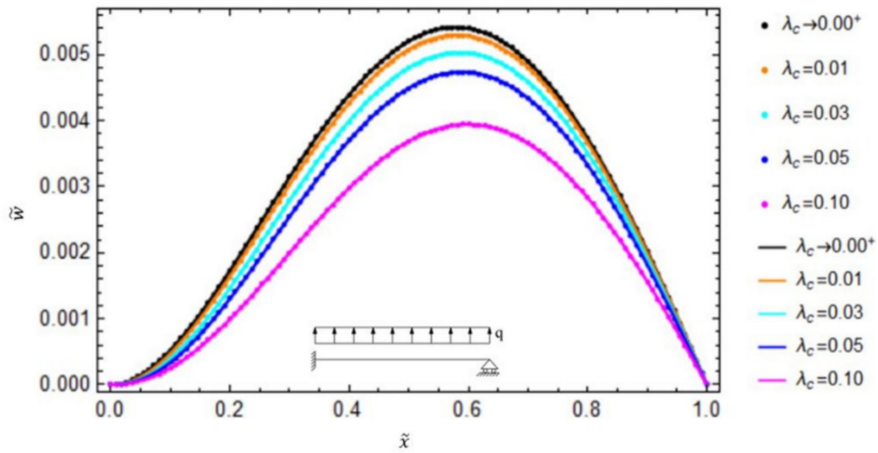

FIGURE 25: Comparison of analytical and the FEM results (Mesh 2) in terms of the dimensionless nonlocal deflection for different values of the nonlocal parameter and for the case of C-P,q

FEM, finite element method

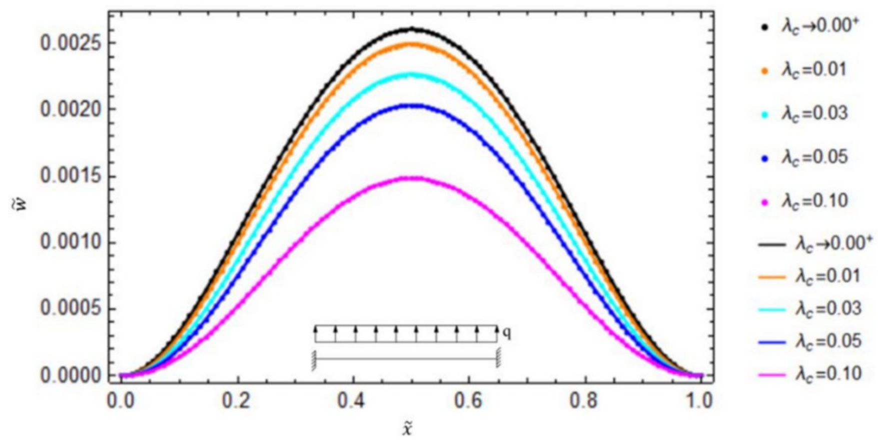

FIGURE 26: Comparison of analytical and the FEM results (Mesh 2) in terms of the dimensionless nonlocal deflection for different values of the nonlocal parameter and for the case of C-C,q

FEM, finite element method

As shown in Tables *4*-*7* and Figures *17*-*26*, as the nonlocal parameter increases, the deflection consistently decreases. In particular, both analytical and FEM approaches exhibit a stiffening behavior as the nonlocal parameter increases. Furthermore, as expected, refining the mesh results in solutions that are closer to the closed-form ones. Additionally, Tables *4*-*7* indicate that the percentage difference, Δ (%), between the results obtained with the SDM model and the FEM approach is very low for all investigated nonlocal parameter values. It is also evident that the errors decrease as the mesh resolution increases; specifically, the errors are always less than 4% for Mesh 1 and less than 1% for Mesh 2. This suggests that both methods yield very similar results and FEM approach can therefore be considered reliable for this type of analysis on the deflection of nanobeams.

Conclusions

In this work, the bending response of Bernoulli-Euler nanobeams was examined using a FEM approach developed with the advanced computational software Comsol Multiphysics® 6.2.

Subsequently, the results were successfully compared with those available in the literature by using the pure nonlocal Stress-Driven Model of elasticity.

Specifically, five different structural schemes of nanobeams, with square cross-section, were considered corresponding to the following different boundary conditions including Cantilever nanobeam subjected to a concentrated force at the free end, Cantilever nanobeam subjected to a uniformly distributed transverse load, Simply-Supported nanobeam subjected to a uniformly distributed transverse load, Clamped-Pinned nanobeam subjected to a uniformly distributed transverse load, and Clamped-Clamped nanobeam subjected to a uniformly distributed transverse load.

Moreover, a comparison between the results of the present work and the experimental results was presented to validate the proposed FEM approach.

The main results of this work can be summarized as follows:

- as the nonlocal parameter increases, the dimensionless nonlocal deflection derived from finite element approach decreases; therefore, the FEM results are able to capture the stiffening behavior of the nanobeam;

- the FEM approach based on identifying the elastic modulus multiplier function accurately approximates both the trend and the numerical value of the analytical solution;

- in the FEM approach, the result is influenced by the type of mesh used. Specifically, as the number of finite elements increases, the difference between the FEM results and the analytical solution decreases;

- the precision of the analysis shown by the very low Δ (%) values confirms the validity of the FEM approach for preliminary design studies and rapid simulations.

In conclusion, this study focused on relatively simple static schemes, such as a cantilever nanobeam subjected to a concentrated load and a Simply-Supported nanobeam subjected to a transverse uniformly distributed load, which are among the most commonly used in the design of mass sensors, accelerometers, and microresonators in NEMS and MEMS devices. The goal was to provide a simple framework, implementable in commercial software, that can effectively capture the nonlocal effects characteristic of nanostructures. For future developments, we plan to extend the method to more complex multidimensional geometries, incorporate advanced physical phenomena such as hygrothermal loading and electrical coupling, and address dynamic vibration analysis to further expand the design and optimization capabilities of nanoelectronic and nanomechanical devices.

Therefore, the obtained results show how the proposed approach is able to capture the small-scale effects of Bernoulli-Euler nanobeams and represents a benchmark for engineering and researchers engaged in the design of nano-scaled structures such as nano-electromechanical systems and biosensors through the use of commercial software.

Appendices

Elastic modulus multiplier functions, f_E, are listed below for cantilever nanobeam subject to concentrated force at the free end and for cantilever, simply-simply, clamped-pinned and clamped-clamped nanobeams subject to a transverse uniformly distributed load.

- S1: Cantilever nanobeam subjected to concentrated force at the free end (C-F,F)

$$f_E = \frac{2e^{\frac{1}{\lambda_c}+\frac{x}{L\lambda_c}}(L-x)E}{2e^{\frac{1}{\lambda_c}+\frac{x}{L\lambda_c}}L - e^{\frac{1}{\lambda_c}}L - 2e^{\frac{1}{\lambda_c}+\frac{x}{L\lambda_c}}x - e^{\frac{1}{\lambda_c}}L\lambda_c + e^{\frac{2x}{L\lambda_c}}L\lambda_c} \qquad (A1)$$

- S2: Cantilever nanobeam subjected to a transverse uniformly distributed load (C-F,q)

$$f_E = -\frac{2e^{\frac{1}{\lambda_c}+\frac{x}{L\lambda_c}}(L-x)^2E}{D_1(x,L,\lambda_c)} \qquad (A2)$$

$$D_1(x,L,\lambda_c) = \begin{bmatrix} -2e^{\frac{1}{\lambda_c}+\frac{x}{L\lambda_c}}L^2 + e^{\frac{1}{\lambda_c}}L^2 + 4e^{\frac{1}{\lambda_c}+\frac{x}{L\lambda_c}}Lx - 2e^{\frac{1}{\lambda_c}+\frac{x}{L\lambda_c}}x^2 + \\ +2e^{\frac{1}{\lambda_c}}L^2\lambda_c - 4e^{\frac{1}{\lambda_c}+\frac{x}{L\lambda_c}}L^2\lambda_c^2 + 2e^{\frac{1}{\lambda_c}}L^2\lambda_c^2 + 2e^{\frac{2x}{L\lambda_c}}L^2\lambda_c^2 \end{bmatrix} \qquad (A3)$$

- S3: Simply-supported nanobeam subjected to a transverse uniformly distributed load (S-S,q)

$$f_E = \frac{2e^{\frac{1}{\lambda_c}+\frac{x}{L\lambda_c}}(L-x)xE}{2e^{\frac{1}{\lambda_c}+\frac{x}{L\lambda_c}}Lx - 2e^{\frac{1}{\lambda_c}+\frac{x}{L\lambda_c}}x^2 + e^{\frac{1}{\lambda_c}}L^2\lambda_c^2 + e^{\frac{2x}{L\lambda_c}}L^2\lambda_c - 4e^{\frac{1}{\lambda_c}+\frac{x}{L\lambda_c}}L^2\lambda_c^2 + 2e^{\frac{2x}{L\lambda_c}}L^2\lambda_c^2} \qquad (A4)$$

- S4: Clamped-pinned nanobeam subjected to a transverse uniformly distributed load (C-P,q)

$$f_E = \frac{-E\lambda_c(L^2-5Lx+4x^2)(-6\lambda_c^3 e^{\frac{1}{\lambda_c}} + 6\lambda_c^3 + 6\lambda_c^2 + 3\lambda_c e^{\frac{1}{\lambda_c}} - 2e^{\frac{1}{\lambda_c}})e^{\frac{L+x}{L\lambda_c}}}{D_2(x,L,\lambda_c)} \qquad (A5)$$

with

$$D_2(x,L,\lambda_c) = \begin{bmatrix} -24L^2\lambda_c^5 e^{\frac{2}{\lambda_c}} + 24L^2\lambda_c^5 e^{\frac{1}{\lambda_c}} + 24L^2\lambda_c^5 e^{\frac{2x}{L\lambda_c}} - 48L^2\lambda_c^5 e^{\frac{L+x}{L\lambda_c}} + \\ +24L^2\lambda_c^5 e^{\frac{2L+x}{L\lambda_c}} - 24L^2\lambda_c^4 e^{\frac{2}{\lambda_c}} + 48L^2\lambda_c^4 e^{\frac{1}{\lambda_c}} + 24L^2\lambda_c^4 e^{\frac{2x}{L\lambda_c}} + \\ -48L^2\lambda_c^4 e^{\frac{L+x}{L\lambda_c}} + 6L^2\lambda_c^3 e^{\frac{2}{\lambda_c}} + 30L^2\lambda_c^3 e^{\frac{1}{\lambda_c}} + 6L^2\lambda_c^3 e^{\frac{2x}{L\lambda_c}} + \\ -18L^2\lambda_c^3 e^{\frac{L+x}{L\lambda_c}} + 4L^2\lambda_c^2 e^{\frac{2}{\lambda_c}} + 6L^2\lambda_c^2 e^{\frac{1}{\lambda_c}} - 12L^2\lambda_c^2 e^{\frac{L+x}{L\lambda_c}} + \\ -2L^2\lambda_c^2 e^{\frac{L+2x}{L\lambda_c}} + 4L^2\lambda_c^2 e^{\frac{2L+x}{L\lambda_c}} - 5L^2\lambda_c e^{\frac{2}{\lambda_c}} - 3L^2\lambda_c e^{\frac{L+2x}{L\lambda_c}} + \\ -L^2 e^{\frac{2}{\lambda_c}} + 2L^2 e^{\frac{2L+x}{L\lambda_c}} + 48L\lambda_c^3 x e^{\frac{L+x}{L\lambda_c}} - 48L\lambda_c^3 x e^{\frac{2L+x}{L\lambda_c}} + \\ +36L\lambda_c^2 x e^{\frac{L+x}{L\lambda_c}} + 12L\lambda_c^2 x e^{\frac{2L+x}{L\lambda_c}} + 12L\lambda_c x e^{\frac{2L+x}{L\lambda_c}} + \\ -10Lxe^{\frac{2L+x}{L\lambda_c}} - 24\lambda_c^3 x^2 e^{\frac{L+x}{L\lambda_c}} + 24\lambda_c^3 x^2 e^{\frac{2L+x}{L\lambda_c}} + \\ -24\lambda_c^2 x^2 e^{\frac{L+x}{L\lambda_c}} - 12\lambda_c x^2 e^{\frac{2L+x}{L\lambda_c}} + 8x^2 e^{\frac{2L+x}{L\lambda_c}} \end{bmatrix} \qquad (A6)$$

- S5: Clamped-clamped nanobeam subjected to a transverse uniformly distributed load (C-C,q)

$$f_E = \frac{2e^{\frac{1}{\lambda_c}+\frac{x}{L\lambda_c}}(L^2-6Lx+6x^2)E(-e^{\frac{1}{\lambda_c}} - \lambda_c + e^{\frac{1}{\lambda_c}}\lambda_c)}{D_3(x,L,\lambda_c)} \qquad (A7)$$

$$D_3(x,L,\lambda_c) = \begin{bmatrix} 2e^{\frac{1}{\lambda_c}+\frac{x}{L\lambda_c}}L^2 + e^{\frac{1}{\lambda_c}}L^2 + e^{\frac{2x}{L\lambda_c}}L^2 + \\ +12e^{\frac{1}{\lambda_c}+\frac{x}{L\lambda_c}}Lx - 12e^{\frac{1}{\lambda_c}+\frac{x}{L\lambda_c}}x^2 + 6e^{\frac{1}{\lambda_c}+\frac{x}{L\lambda_c}}x^2\lambda_c + \\ -12e^{\frac{x}{L\lambda_c}}x^2\lambda_c - 12e^{\frac{1}{\lambda_c}+\frac{x}{L\lambda_c}}L^2\lambda_c^{2+12e^{\frac{x}{L\lambda_c}}}L^2\lambda_c^2 \end{bmatrix} \qquad (A8)$$

Additional Information

Author Contributions

All authors have reviewed the final version to be published and agreed to be accountable for all aspects of the work.

Concept and design: Giuseppe Lovisi, Luciano Feo, Rosa Penna, Gerarda Landi

Acquisition, analysis, or interpretation of data: Giuseppe Lovisi, Rosa Penna, Gerarda Landi

Drafting of the manuscript: Giuseppe Lovisi, Luciano Feo, Rosa Penna, Gerarda Landi

Critical review of the manuscript for important intellectual content: Giuseppe Lovisi, Luciano Feo, Rosa Penna, Gerarda Landi

Supervision: Luciano Feo, Rosa Penna

Disclosures

Human subjects: All authors have confirmed that this study did not involve human participants or tissue. **Animal subjects:** All authors have confirmed that this study did not involve animal subjects or tissue. **Conflicts of interest:** In compliance with the ICMJE uniform disclosure form, all authors declare the following: **Payment/services info:** All authors have declared that no financial support was received from any organization for the submitted work. **Financial relationships:** All authors have declared that they have no financial relationships at present or within the previous three years with any organizations that might have an interest in the submitted work. **Other relationships:** All authors have declared that there are no other relationships or activities that could appear to have influenced the submitted work.

Acknowledgements

The authors sincerely acknowledge the financial support provided by the Italian Ministry of University and

Research (MUR). This work was funded through the Research Grant PRIN 2020 (No. 2020EBLPLS) for the project "Opportunities and Challenges of Nanotechnology in Advanced and Green Construction Materials." Additional support was received from the National Recovery and Resilience Plan (NRRP), Mission 4, Component 2, Investment 1.1, under Call for Tender No. 104 (published on 02/02/2022 by MUR), financed by the European Union – NextGenerationEU for the project "Intelligent Systems for Infrastructural Diagnosis in Smart Concrete (ISIDE)" (Grant No. 2022S88WAY, CUP D53D23008820006).

References

1. Civalek Ö, Uzun B, Yaylı MÖ: On nonlinear stability analysis of saturated embedded porous nanobeams. International Journal of Engineering Science. 2023, 190:103898. 10.1016/j.ijengsci.2023.103898
2. Li J, Li S, Ma Q: Active tuning of size-dependent band gaps of functionally graded porous phononic beam at nanoscale. Applied Mathematical Modelling. 2025, 140:115891. 10.1016/j.apm.2024.115891
3. Dhore N, Khalsa L, Varghese V: Hygrothermoelastic analysis of the nano-circular plate with memory effect. Applied Mathematical Modelling. 2025, 138:115797. 10.1016/j.apm.2024.115797
4. Koç MA, Esen İ, Eroğlu M: The effects of Casimir, van der Waals and electrostatic forces on the response of nanosensor beams. Applied Mathematical Modelling. 2024, 129:297-320. 10.1016/j.apm.2024.02.002
5. Xu X, Shahsavari D, Karami B: On the forced mechanics of doubly-curved nanoshell. International Journal of Engineering Science. 2021, 168:103538. 10.1016/j.ijengsci.2021.103538
6. Su JY, Huang XQ, Xu HL, Zhou JY, Meng ZM: Ultrafast all-optical switching in a silicon-polymer compound slotted photonic crystal nanobeam cavity. Optical Review. 2022, 30:33-40. 10.1007/s10043-022-00779-4
7. Li Q, Zhang H: Influence of surface effect on post-buckling behavior of graded porous nanobeam subjected to follower force. Microsystem Technologies. 2023, 29:779-91. 10.1007/s00542-023-05458-1
8. Chen CQ, Shi Y, Zhang YS, Zhu J, Yan YJ: Size dependence of Young's Modulus in ZnO nanowires. Physical Review Letters. 2006, 96:075505. 10.1103/physrevlett.96.075505
9. Chen AL, Wang YS: Size-effect on band structures of nanoscale phononic crystals. Physica E Low-dimensional Systems and Nanostructures. 2011, 44:317-21. 10.1016/j.physe.2011.08.032
10. Stan G, Ciobanu CV, Parthangal PM, Cook R: Diameter--dependent radial and tangential elastic moduli of ZnO nanowires. Nano Letters. 2007, 7:3691-697. 10.1021/nl071986e
11. Agrawal R, Peng B, Gdoutos EE, Espinosa HD: Elasticity size effects in ZnO nanowires−a combined experimental-computational approach. Nano Letters. 2008, 8:3668-674. 10.1021/nl801724b
12. Zhang Y, Hong J, Liu B, Fang D: Strain effect on ferroelectric behaviors of BaTiO3 nanowires: a molecular dynamics study. Nanotechnology. 2010, 21:015701. 10.1088/0957-4484/21/1/015701
13. Li C, Lai SK, Yang X: On the nano-structural dependence of nonlocal dynamics and its relationship to the upper limit of nonlocal scale parameter. Applied Mathematical Modelling. 2019, 69:127-41. 10.1016/j.apm.2018.12.010
14. Eringen AC: Linear theory of nonlocal elasticity and dispersion of plane waves. International Journal of Engineering Science. 1972, 10:425-35. 10.1016/0020-7225(72)90050-x
15. Eringen AC: On differential equations of nonlocal elasticity and solutions of screw dislocation and surface waves. Journal of Applied Physics. 1983, 54:4703-710. 10.1063/1.332803
16. Martin O: Nonlocal effects on the dynamic analysis of a viscoelastic nanobeam using a fractional Zener model. Applied Mathematical Modelling. 2019, 73:637-50. 10.1016/j.apm.2019.04.029
17. Zhang H, Wang CM, Challamel N, Pan WH: Calibration of Eringen's small length scale coefficient for buckling circular and annular plates via Hencky bar-net model. Applied Mathematical Modelling. 2020, 78:399-417. 10.1016/j.apm.2019.09.052
18. Attia MA, Matbuly MS, Osman T, AbdElkhalek M: Dynamic analysis of double cracked bi-directional functionally graded nanobeam using the differential quadrature method. Acta Mechanica. 2024, 235:1961-2012. 10.1007/s00707-023-03797-8
19. Karmakar S, Chakraverty S: Vibration of a piezoelectric nanobeam with flexoelectric effects by Adomian decomposition method. Acta Mechanica. 2023, 234:2445-460. 10.1007/s00707-023-03512-7
20. Zaera R, Serrano Ó, Fernandez-Saez J: On the consistency of the nonlocal strain gradient elasticity. International Journal of Engineering Science. 2019, 138:65-81. 10.1016/j.ijengsci.2019.02.004
21. Benvenuti E, Simone A: One-dimensional nonlocal and gradient elasticity: Closed-form solution and size effect. Mechanics Research Communications. 2013, 48:46-51. 10.1016/j.mechrescom.2012.12.001
22. Fernandez-Saez J, Zaera R, Loya JA, Reddy JN: Bending of Euler-Bernoulli beams using Eringen's integral formulation: A paradox resolved. International Journal of Engineering Science. 2016, 99:107-16. 10.1016/j.ijengsci.2015.10.013
23. Romano G, Barretta R: Comment on the paper "Exact solution of Eringen's nonlocal integral model for bending of Euler-Bernoulli and Timoshenko beams" by Meral Tuna & Mesut Kirca. International Journal of Engineering Science. 2016, 109:240-42. 10.1016/j.ijengsci.2016.09.009
24. Romano G, Barretta R, Diaco M, de Sciarra FM: Constitutive boundary conditions and paradoxes in nonlocal elastic nanobeams. International Journal of Mechanical Sciences. 2017, 121:151-56. 10.1016/j.ijmecsci.2016.10.036
25. Barretta R, Luciano R, de Sciarra FM, Vaccaro MS: Modelling issues and advances in nonlocal beams mechanics. International Journal of Engineering Science. 2024, 198:104042. 10.1016/j.ijengsci.2024.104042
26. Romano G, Barretta R: Nonlocal elasticity in nanobeams: the stress-driven integral model. International Journal of Engineering Science. 2017, 115:14-27. 10.1016/j.ijengsci.2017.03.002
27. Barretta R, Canadija M, Feo L, Luciano R, de Sciarra FM, Penna R: Exact solutions of inflected functionally graded nano-beams in integral elasticity. Composites Part B Engineering. 2018, 142:273-86. 10.1016/j.compositesb.2017.12.022
28. Song ZW, Lai SK, Lim CW: On the nature of constitutive boundary and interface conditions in stress-driven nonlocal integral model for nanobeams. Applied Mathematical Modelling. 2025, 144:115949. 10.1016/j.apm.2025.115949
29. Vaccaro MS, Barretta R, de Sciarra FM, Reddy JN: Nonlocal integral elasticity for third-order small-scale beams.

Acta Mechanica. 2022, 233:2393-403. 10.1007/s00707-022-03210-w
30. Ren YM, Qing H: Bending and buckling analysis of functionally graded Euler-Bernoulli beam using stress-driven nonlocal integral model with bi-Helmholtz kernel. International Journal of Applied Mechanics. 2021, 13:2150041. 10.1142/s1758825121500411
31. Lam DCC, Yang F, Chong ACM, Wang J, Tong P: Experiments and theory in strain gradient elasticity. Journal of the Mechanics and Physics of Solids. 2003, 51:1477-508. 10.1016/s0022-5096(03)00053-x
32. Darban H, Luciano R, Basista M: Calibration of the length scale parameter for the stress-driven nonlocal elasticity model from quasi-static and dynamic experiments. Mechanics of Advanced Materials and Structures. 2022, 30:3518-524. 10.1080/15376494.2022.2077488
33. Apuzzo A, Bartolomeo C, Luciano R, Scorza D: Novel local/nonlocal formulation of the stress-driven model through closed form solution for higher vibrations modes. Composite Structures. 2020, 252:112688. 10.1016/j.compstruct.2020.112688
34. Vaccaro MS, de Sciarra FM, Barretta R: On the regularity of curvature fields in stress-driven nonlocal elastic beams. Acta Mechanica. 2021, 232:2595-603. 10.1007/s00707-021-02967-w
35. Guo Y, Alam M: Nonlinear bending and thermal postbuckling of magneto-electro-elastic nonlocal strain-gradient beam including surface effects. Applied Mathematical Modelling. 2025, 142:115955. 10.1016/j.apm.2025.115955
36. Ussorio D, Vaccaro MS, Barretta R, Luciano R, de Sciarra FM: Large deflection of a nonlocal gradient cantilever beam. International Journal of Engineering Science. 2025, 206:104172. 10.1016/j.ijengsci.2024.104172
37. Barretta R, Canadija M, Luciano R, de Sciarra FM: On the mechanics of nanobeams on nano-foundations. International Journal of Engineering Science. 2022, 180:103747. 10.1016/j.ijengsci.2022.103747
38. Vaccaro MS: On geometrically nonlinear mechanics of nanocomposite beams. International Journal of Engineering Science. 2022, 173:103653. 10.1016/j.ijengsci.2022.103653
39. Penna R, Lambiase A, Lovisi G, Feo L: Investigating hygrothermal bending behavior of FG nanobeams via local/nonlocal stress gradient theory of elasticity with general boundary conditions. Mechanics of Advanced Materials and Structures. 2023, 31:9260-269. 10.1080/15376494.2023.2269938
40. Barretta R, Iuorio A, Luciano R, Vaccaro MS: On wave propagation in nanobeams. International Journal of Engineering Science. 2024, 196:104014. 10.1016/j.ijengsci.2023.104014
41. Barretta R, Iuorio A, Luciano R, Vaccaro MS: Wave solutions in nonlocal integral beams. Continuum Mechanics and Thermodynamics. 2024, 36:1607-627. 10.1007/s00161-024-01319-y
42. Penna R: Bending analysis of functionally graded nanobeams based on stress-driven nonlocal model incorporating surface energy effects. International Journal of Engineering Science. 2023, 189:103887. 10.1016/j.ijengsci.2023.103887
43. Gurtin ME, Murdoch I: A continuum theory of elastic material surfaces. Archive for Rational Mechanics and Analysis. 1975, 57:291-323. 10.1007/bf00261375
44. Gurtin ME, Murdoch I: Surface stress in solids. International Journal of Solids and Structures. 1978, 14:431-40. 10.1016/0020-7683(78)90008-2
45. Lovisi G: Application of the surface stress-driven nonlocal theory of elasticity for the study of the bending response of FG cracked nanobeams. Composite Structures. 2023, 324:117549. 10.1016/j.compstruct.2023.117549
46. Feo L, Lovisi G, Penna R: Free vibration analysis of functionally graded nanobeams based on surface stress-driven nonlocal model. Mechanics of Advanced Materials and Structures. 2023, 31:10391-399. 10.1080/15376494.2023.2289079
47. Lovisi G, Feo L, Lambiase A, Penna R: Application of surface stress-driven model for higher vibration modes of functionally graded nanobeams. Nanomaterials. 2024, 14:350. 10.3390/nano14040350
48. Penna R, Lovisi G, Feo L: Buckling analysis of functionally graded nanobeams via surface stress-driven model. International Journal of Engineering Science. 2024, 205:104148. 10.1016/j.ijengsci.2024.104148
49. Eltaher MA, Emam SA, Mahmoud FF: Free vibration analysis of functionally graded size-dependent nanobeams. Applied Mathematics and Computation. 2012, 218:7406-420. 10.1016/j.amc.2011.12.090
50. Aria AI, Friswell M: A nonlocal finite element model for buckling and vibration of functionally graded nanobeams. Composites Part B Engineering. 2019, 166:233-46. 10.1016/j.compositesb.2018.11.071
51. Srividhya S, Raghu P, Rajagopal A, Reddy JN: Nonlocal nonlinear analysis of functionally graded plates using third-order shear deformation theory. International Journal of Engineering Science. 2018, 125:1-22. 10.1016/j.ijengsci.2017.12.006
52. Raghu P, Rajagopal A, Reddy JN: Nonlocal nonlinear finite element analysis of composite plates using TSDT. Composite Structures. 2018, 185:38-50. 10.1016/j.compstruct.2017.10.075
53. Bacciocchi M, Fantuzzi N, Ferreira AJM: Static finite element analysis of thin laminated strain gradient nanoplates in hygro-thermal environment. Continuum Mechanics and Thermodynamics. 2020, 33:969-92. 10.1007/s00161-020-00940-x
54. Pinnola FP, Vaccaro MS, Barretta R, de Sciarra FM: Finite element method for stress-driven nonlocal beams. Engineering Analysis with Boundary Elements. 2022, 134:22-34. 10.1016/j.enganabound.2021.09.009